Unveiling the catalytic effects of Brønsted acidic ionic liquid on quantitative α -glucose conversion to 5-HMF: Experimental and computational studies

Yusif Abdullayev*^[a,b], Orkhan Ahmadov^[a], Gunay Valadova^[a,b], Ayan Karimli^[a], and Jochen Autschbach^[c]

- [a] Department of Chemical Engineering, Baku Engineering University, Hasan Aliyev str. 120, Baku, Absheron, AZ0101, Azerbaijan. Email: yabdullayev@beu.edu.az
- 7 [b] Institute of Petrochemical Processes, Azerbaijan National Academy of Sciences, Khojaly ave. 30, Az1025, Baku, Azerbaijan
- 9 [c] Department of Chemistry, University at Buffalo, State University of New York, Buffalo, New York 14260-3000, United States.

1112 Abstract

Effective biomass conversion to 5-HMF(5-hydroxymethylfurfural) is still a challenge and needs to be improved because of the 5-HMF importance as building blocks for valuable monomers and fuel precursors. We suggest for the first time utilization of low-cost metal-free Brønsted acidic lonic liquid (IL) N,N-Diethyl-1,4-phenylenediamine hydrogen sulfate, [DPhDA]HSO₄ as a catalyst for the α-glucose dehydration to 5-HMF. Quantitative α-glucose conversion is achieved via optimizing the reaction condition: 91.4 % 5-HMF yield with 30 mol% [DPhDA]HSO₄ in the presence of DMSO as a solvent at 160 °C in 30 minutes (TOF 6.1 h⁻¹). 3-fold increase in reaction time leads to higher (94%) 5-HMF yield at 160 °C with lower TOF 1.6 h⁻¹. The IL surprising catalytic performance is scrutinized with its amphiprotic nature (availability of basic and acidic spots in its structure (Figure 1)). Further computational mechanistic studies revealed the function of the catalytic sites in the α-glucose dehydration. We calculated five-membered ring formation and water extrusion in one concerted transition state (TS2A, Δ G[‡]=38.8 kcal/mol) following the α-glucose ring-opening (TS1, Δ G[‡]=20.4 kcal/mol). Further four steps (sp³-s, C-H bond cleavages (TS3, TS6) and dehydroxylation (TS4A, TS5)) are quite straightforward to reach the product (5-HMF).

Keywords: ionic liquid, catalyst, 5-HMF, DFT, transition state, α -glucose

1. INTRODUCTION

Conversion of biomass to 5-HMF [1, 2] and biodiesel [3] has been studied extensively because of the prospective fossil fuel shortage and high demand of the world growing population for chemicals from sustainable sources. Some derivatives of 5-HMF (e.g., dimethylfuran, ethoxymethylfurfural) have advantages over fossil-derived fuel such as high octane rating, energy-dense, and carbon-neutral [4, 5]. 5-HMF is also very important building blocks for the production of versatile chemicals (1,6-hexanediol[6], 5-hydroxymethyl-2-furancarboxylic acid [7], 2,5-furan dicarboxylic acid [8], polyethylene furanoate (PEF) [9]). It is enormously important to decrease carbon footprint by replacing monomer (e.g., terephthalic acid with 2,5-furan dicarboxylic acid) that comes from fossil resources with 5-HMF derivatives resulted in the generation of sustainable alternative (PEF) of polyethylene terephthalate (PET). Accordingly, research on the facile and effective conversion of biomass to 5-HMF has great importance.

We chose glucose as a starting material for 5-HMF synthesis in this study since it is one of the most abundant carbohydrates in nature. It is available in many fruits and as a monomer of polysaccharide, i.e., cellulose, starch, and amylopectin. Screening of studies show that conversion of biomass was conducted

mostly by the catalyst-free thermal means [10, 11], heterogeneous catalysis [12, 13], and the Lewis acidic metal salts catalysis [14, 15]. CrCl₃ promoted synthesis of 5-HMF with 71.3% yield from glucose was conducted in the presence of the 1-butyl-3-methylimidazolium chloride IL [16]. CrCl₃ with IL co-catalysts (N-methyl-2-pyrrolidone hydrogen sulfate, N-methyl-2-pyrrolidone bromide, N-methyl-2-pyrrolidone chloride) were employed for the synthesis of 5-HMF from glucose in the N,N-dimthethylacetamide solvent [17]. It was found that the utilization of DMSO as a solvent with the proposed catalytic system lowered the conversion of glucose and the yield of 5-HMF because it binds CrCl₃ and forms six-coordinated structure according to the DFT (Density Functional theory) calculations. CrCl2 was found to be a more efficient catalyst than CrCl₃ in the presence of co-catalyst (tetraethylammonium chloride) and solvent (DMSO) for 5-HMF production with 54.8% yield from glucose [18]. CrCl₃ was also taken without any cocatalyst for 5-HMF (71% yield) synthesis from glucose in an IL (1-butyl-3-methyl imidazolium chloride) solvent [19, 20]. The 1-butyl-3-methylimidazolium hydrogen sulfate-AlCl₃ catalytic system was utilized for the direct 5-ethoxymethylfurfural (5-EMF) synthesis from glucose with 37% yield [21]. AlCl₃-H₂O/THF biphasic system was taken to produce 5-HMF from glucose with 62% yield in the presence of 0.1 M HCl [22]. AICl₃ was also exploited for mixed 5-HMF and 5-EMF synthesis in ethanol/water solvent system [23]. The consumption of chromium, aluminum, iron, and tin salts are not desired even though the process is carbon-neutral because of environmental concerns. As mentioned, ILs are used as a solvent or co-catalyst for biomass dehydration processes traditionally.

Extensive IL consumption as a solvent is not economically viable since the IL high viscosity at a lower temperature, making a separation process challenging in the industry [24]. As seen from the above studies, the utilization of chromium salts in the presence of IL solvents results in lower or moderate 5-HMF yield. We achieved a near-quantitative 5-HMF yield (94%) without using toxic metal salts with the consumption of the catalytic amount of IL ([DPhDA]HSO₄). Despite the IL application as a catalyst is "greener", a few studies were carried out by metal-free IL catalysts promoted biomass conversion to 5-HMF. 1-hydroxyethyl-3-methylimidazolium tetrafluoroborate was taken as a catalyst for the conversion of glucose and fructose to 5-HMF without using any Lewis acidic co-catalysts in the presence of DMSO with 67% yield [25]. Metal functionalized IL (1-sulfonic acid-3-methyl imidazolium tetrachlo-roferrate) was utilized for the same purpose which yielded lower 5-HMF (18%) and moderate levulinic acid (LA) (68%) from glucose conversion in harsh condition [26]. Polyethylene supported IL was applied as a catalyst for fructose dehydration to 5-HMF with 86% yield [27]. As seen from the above literature studies, usage of IL for the 5-HMF production requires improvements (because of lower or moderate 5-HMF yield) for the industrial-scale application.

Due to the significance of biomass valorization, computational studies were applied to rationalize the reaction mechanism: 1-butyl-3-methyl-imidazolium bromide catalyzed fructose dehydration to 5-HMF was studied computationally [28, 29]. Glycosidic bond cleavage of cellobiose and cellulose were investigated computationally via applying alkali/alkaline-earth metals as a catalyst and in catalyst-free condition [30, 31]. Detailed mechanistic *ab-initio* studies were performed for Al(OMe)₃-catalyzed conversion of glucose to 5-HMF in which very long mechanistic route is proposed: Three consecutive transition states (TS) for glucose ring-opening, additional three TSs for isomerization from the open-chain glucose to the open-chain fructose isomer, two more TSs for ring closure and six TSs for the dehydration of fructose to 5-HMF [32].

The aforementioned computational studies unnecessarily recommended very long mechanistic routes for the studied reaction. We proposed alternative mechanistic DFT studies for the glucose

conversion to 5-HMF (see Section 4.6) via a shorter route (only six TSs required to reach the product). Unlike the previous IL incorporated mechanistic investigations, we unveiled the IL cation and anion components dual catalytic influences on the glucose dehydration reaction. The IL inactive involvement (catalyst-free) in the mechanism was also presented, which allows for a better interpretation of the IL catalytic behaviors.

Herein, we report a new "greener" protocol for selective dehydration of glucose to 5-HMF with quantitative yield (94%) via applying superior IL catalyst (N,N-Diethyl-1,4-phenylenediamine hydrogen sulfate, [DPhDA]HSO₄) without co-catalyst in the presence of DMSO as a solvent. Surprisingly, we achieved

such a high yield of 5-HMF with the low-cost IL catalyst in the metal-free condition, which is not possible with the toxic metal-containing environmentally non-benign catalytic systems, as mentioned above. The attractive result inspired us to investigate the catalyst structure (Figure 1) deeply. Natural bond orbital (NBO) charge distribution of the DFT optimized structure of the IL implies the existence of the three catalytic centers (circled green in the caption, Figure 1) in the IL structure: tertiary amine (Et₂N-Ph), primary alkyl ammonium (Ph-NH₃⁺), and HO- of the anion part (HSO₄⁻). Based on the charge analysis, the cation part (Ph-NH₃⁺) may act the same as the anion part in terms of acidity because of the same charge of protons (+0.51). The catalytic activity of the tertiary amine (Et₂N-Ph) part was scrutinized in Section 4.6. Because of basicity, this part

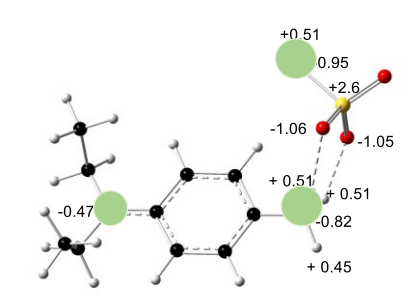


Figure 1. DFT calculated NBO charge distribution of [DPhDA]HSO₄ (C, black; N, blue; O, red; H, grey; S, yellow).

easily involves in proton abstraction and subsequent dehydration. Due to the lower basicity (-0.47) and steric hindrance of Et_2N -Ph, HSO_4^- binds to Ph-NH₃⁺(-0.82). The IL anion part (HSO_4^-) catalytic role in dehydration was well studied in our previous works [33, 34]. The peculiarity (availability of acid/base pairs) of the IL is related to its cation part, which makes it a more efficient catalyst.

2. EXPERIMENTAL SECTION

2.1 Materials and Instruments. DMSO (99.9%), N,N-dimethylacetamide (DMA, 99%), diethyl ether (99%), 1,4-dioxan (100%) N,N-diemthylformamide (DMF, 99%) were purchased from VWR. [DPhDA]HSO₄ (97%), aniline sulfate [An]₂SO₄ (98%), aluminum ammonium sulfate dodecylhydrate AlNH₄(SO₄)₂·12H₂O (reagent grade, crystalline), copper sulfate pentahydtate CuSO₄·5H₂O (99%), aluminum sulfate-18-hydrate Al₂(SO₄)₃·18H₂O (99%), cobalt (III) chloride hexahydrate CoCl₃·6H₂O (99%), chromium (III) chloride hexahydrate CrCl₃·6H₂O (98%), 18-crown-6 (99%), ammonium monohydrogen phosphate (NH₄)₂HPO₄ (97%) were provided from Alfa Aesar. 3,3'-Diaminobenzidine tetrahydrochloride, [(NH₃)₂C₆H₃]₂Cl₄ (98%) was supplied from ABCR GmbH. α-glucose was purchased from Arbor Chemicals. Extra pure 5-HMF was provided from TRC Canada for preparing standard solution, which is used in the standard curve method. UV analysis was conducted by UV-visible spectrophotometer (U-2900, HITACHI). IR analysis was performed with Agilent Cary 630 FTIR. NMR spectra were recorded with Bruker 300 MHz NMR instrument.

2.2 5-HMF synthesis and quantification procedure. 1 g anhydrous α -glucose (dried under vacuum at 40°C in 10-15 min), 10 mL DMSO, and 30 mol% catalyst (relative to α -glucose) [DPhDA]HSO₄ were added to a sealed tube. The reaction was conducted in a temperature-controlled oil bath with continuous steering at

400 rpm in the 15-180 minutes time range. The best results were obtained at 160 °C in 30 min. (5-HMF yield: 91.4%) or at 140 °C in 120 min. (5-HMF yield: 94.0%). Then, the reaction mixture was cooled down to room temperature using an ice bath. 0.1 mL sample was taken from the homogeneous mixture and diluted to 500 mL using deionized water. 1 mL aliquot was used from the solution for the 5-HMF yield analysis with the UV-vis standard curve method at 284 nm (See supporting information (SI)). Replicated measurements of the 5-HMF yield on the same solution do not have a noticeable percentage error (±2%). This method was proved to be very reliable for 5-HMF and LA yield calculations relative to the HPLC, GC and NMR analysis [35]. Because of the reaction mixture content (DMSO+Catalyst+5-HMF, trace byproducts), there is a blue shift (275 nm) was observed in the 5-HMF UV signal. The sample was extracted by diethyl ether, and then the solvent was evaporated. Isolated crude 5-HMF (yellow liquid) UV spectrum was recorded. The previous λ_{max} =284 nm was detected, which is noticed in the analytical grade 5-HMF/water solution. Isolated 5-HMF was characterized by NMR and IR (See SI for spectra). Glucose was not observed in the reaction mixture, which is an indication of the quantitative glucose conversion to the products. Trace LA formation was confirmed according to the wavelength (266 nm) with very low absorbance. The reaction mixture turns color to black over time, which shows a small amount of glucose transformation to humin. The 5-HMF yield was calculated according to the following equation (Eq. (1)):

143
$$5 - HMF \ yield \ (\%) = \frac{5 - HMF \ observed \ mol}{\alpha - glucose \ initial \ mol} \cdot 100$$
 Eq. (1)

3. COMPUTATIONAL DETAILS

We utilized the Gaussian 16 software package [36] for the calculations. All the species (reactants, intermediates, and transition state (TS) structures were optimized without geometry constraints, with Kohn-Sham Density Functional Theory (KS-DFT) and the M06-2X functional, which is deemed suitable for an accurate estimation of the energy barriers in biomass conversion reactions [30, 37]. The 6-31G* basis set was used for all (H, C, O, and N) atoms except S. We used the 6-31++G(d,p) basis for sulfur based on our previous studies for optimization of sulfur-containing structures [33]. Since DMSO was utilized experimentally, the self-consistent reaction field (SCRF) with a dielectric constant for DMSO (ϵ =46.7) was applied in all calculations. Minima (no imaginary frequency), saddle points (1 imaginary frequency), and free energies at 393.15 K (same as in most experiments) were identified via frequency calculations. Calculations were also done for the highest temperature (433.15 K) of the experiments to examine the changes in the free energy barriers (Figure 8). Applying high temperature resulted in 11 kcal increase in the rate-controlling step barrier (I1 \rightarrow TS2A). Intrinsic reaction coordinate (IRC) searches were applied to connect transition states (TS) and intermediate/product structures. Total energies, Gibbs energies, enthalpies, and optimized geometries (in xyz format) of all structures are given in (SI).

4. RESULTS AND DISCUSSION

4.1 Catalyst screening for glucose conversion to 5-HMF

We tested various catalytic systems on the glucose dehydration reaction (Figure 2). The catalytic systems are the frequently utilized metal salts (e.g., $CrCl_3$, $CuSO_4$, $Al_2(SO_4)_3$), some ionic liquids, and their combinations with metals salts and the natural tuff mineral. The aim of the comparative catalysts screening is to evaluate Lewis acidic metal salts versus the tested IL catalyst at the same condition. Even though the Lewis acidic catalysts were employed widely for glucose dehydration in the past, it may not be appropriate to arbitrate their catalytic efficiencies if different conditions (e.g., temperature, solvent) are

applied. Yuan et al. reported Cr^{2+} as more effective than Cr^{3+} in the presence of a cocatalyst[18]. Contrary to this study, we found Cr^{3+} as more efficient than Cr^{2+} (without any co-catalyst usage), which can be

167

168

169 170

171

172

173

174

175

176177

178

179

180

181

182

183

184

185

186

187 188

189 190

191

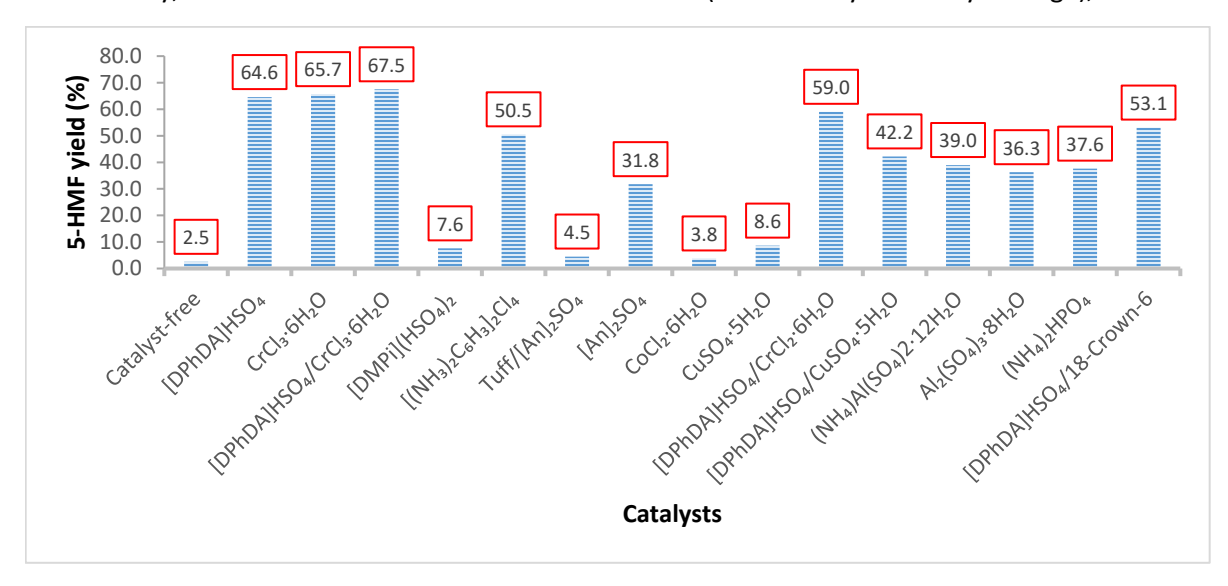


Figure 2. The glucose dehydration reaction condition: 1 g glucose, 30 mol% catalyst relative to glucose, 120 °C, and in 30 min in the presence of DMSO as a solvent.

attributed to the higher Lewis acidity of Cr3+. Catalytic effectiveness of the other metal salts is not satisfactory compared to chromium chlorides on glucose dehydration, which is in good agreement with the previous studies [21]. $[(NH_3)_2C_6H_3]_2Cl_4$ is also seemed efficient (50.5 % 5-HMF yield) than some of the tested metal salts, which can promise perspective in the glucose dehydration to 5-HMF. The study shows that CrCl₃·6H₂O, [DPhDA]HSO₄ (IL), and their combination in the same mol ratio are suitable to reach the satisfactory 5-HMF yield. The surprising result (64.6% 5-HMF yield in 30 minutes with IL catalyst the same as chromium salt) encouraged us to perform further optimizations by changing reaction parameters (e.g., catalyst loading, time, temperature) via using IL catalyst solely. The IL is low-cost and environmentally benign compared to the traditionally utilized chromium salts. The IL is also easily accessible than commonly employed imidazolium-based ILs (as a solvent or co-catalyst) on the glucose dehydration reaction. Mixing the chromium salt and IL mixture is not a good option since only a small increase in the 5-HMF yield was recorded. As seen from Figure 2, we used 18-crown-6 ether at the same mol ratio with the IL catalyst to block the positive pole of the catalyst (-NH₃⁺). A small decrease in the 5-HMF yield (53.7%) relative to the single IL catalyst utilization can be scrutinized with the interaction (strong hydrogen bonds) between the ether oxygen atoms and catalyst positive site. The fact, in turn, supports the synergetic role of the computationally defined catalytic spots (Figure 1). [An]₂SO₄ was employed without a co-catalyst and in the presence of tuff mineral. Both acidic protons of sulfuric acid are trapped with two aniline molecules, which resulted in the formation of two Ph-NH₃⁺ acidic cations (pKa=4.6) and basic SO₄²⁻ anion. The twofold decrease in 5-HMF yield is observed when shifting from [DPhDA]HSO₄ to [An]₂SO₄ can be rationalized by HSO₄-strong acidity (pKa=2.0). Tuff is a porous (see SI for BET surface area analysis) natural mineral that contains catalytically active metals, e.g., Zn, Ni, Ga, Ti in low quantity. We expected to boost the IL catalytic performance because of tuff Lewis acidity, but a considerable decline in 5-HMF yield was noticed upon mixing tuff with [An]₂SO₄. The tuff/IL catalytic system adverse impact on 5-HMF yield can be rationalized with undesired electrostatic interaction between IL and tuff. Tuff contains mainly quartz and aluminum silicates (see SI for XRD spectrum), which may have a considerable role in blocking the IL acidic

protons. The chemisorptive nature of tuff deactivates IL, and therefore, can not be recommended for glucose conversion to 5-HMF. TOF (h⁻¹) values of the tested catalysts in Figure 2 were calculated and described in Figure S23 of SI. Based on the above indepth investigations mentioned, we chose [DPhDA]HSO₄ as a superior catalyst for efficient glucose dehydration to 5-HMF. The FT-IR analysis (Figure 3) was also conducted using fresh and utilized (after 5th reuse, see Section 4.5 for recycle test) IL catalyst [DPhDA]HSO₄. The catalyst primary ammonium (-NH₃⁺) stretching bands

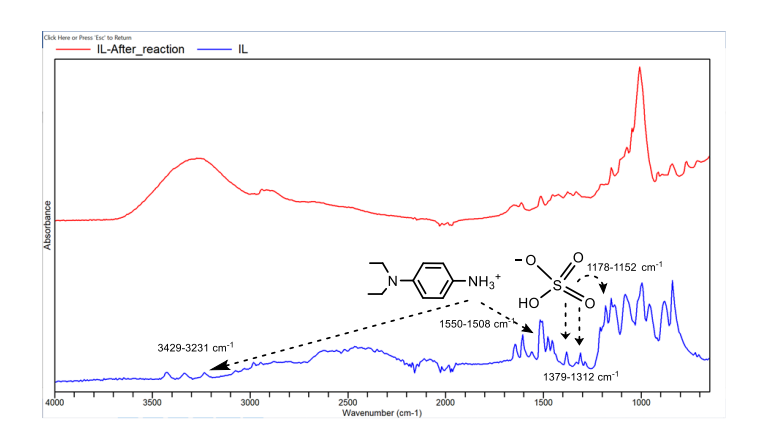


Figure 3. Overlayed IR spectra of fresh (blue) and recycled (red) IL ([DPhDA]HSO₄) catalyst.

correspond to 3429-3231 cm⁻¹ (blue spectrum, fresh catalyst) vanished and converted to broad signal at 3272 cm⁻¹. The primary ammonium cation bending bands appeared near 1550-1508 cm⁻¹. The hydrogen sulfate (S=O) bonds show symmetric and asymmetric stretching bands at 1379-1312 cm⁻¹ and 1178-1152 cm⁻¹. The IR spectra changes imply the deterioration of the anion part (HSO₄⁻¹) of the IL catalyst. The cation component neutralization is proved by bending and stretching bands signal disappearance. HSO₄⁻¹ instability (gradual reduction to SO₂ at a high temperature) was scrutinized in our previous work [34]. The IL catalyst decomposition over time may be responsible for considerable 5-HMF yield decline after 4th resue (Figure 7). The IL catalyst acidity was studied with the Hammett method [38], and 4-nitroaniline was taken as a basic indicator (See SI). The calculated Hammett number (H_o =2.4) indicates the catalyst is weak acidic relative to the traditional ILs utilized as a solvent/catalyst [39]. Because of the additional basic spot (Et₂N-Ph) weak acidity is theoretically expected (Figure 1). The IL superior catalytic effects are not only related to its acidity. The catalyst basic spot also takes part synergetically on glucose dehydration (See Section 4.6).

4.2 Variation of temperature and time

The reaction was carried out at the 100-160 °C temperature range with 30 mol% catalyst loading in 15-180 minutes time range (Figure 4). As seen from the figure, increasing reaction time up to 120 min positively affects the 5-HMF yield in the case reactions carried out at 100-140 °C. The yield slowly goes down beyond 30 min if we heat the reaction mixture to 160 °C. The maximum achievable 5-HMF yield is observed to be 78% at 100 °C in 120 min while the reaction at 120 °C reaches the maximum 5-HMF yield (73.4%) in 90 min. The best reaction condition can be suggested in 30 min at 160 °C and 120 min at 140 °C, which resulted in quantitative 5-HMF yields, 91.4%, and 94.0%, respectively. We calculated turnover frequencies (TOF) to determine the best condition. For both cases (30 min at 160 °C and 120 min at 140 °C) the TOF values are 6.1 h⁻¹ and 1.6 h⁻¹, respectively, which implies the shorter reaction time (30 min) and the higher temperature (160 °C) is a suitable condition for the IL better catalytic efficiency. Shorter reaction time and high temperature were also recommended previously for maximizing 5-HMF yield [1].

Carrying out the reaction at 160 °C for a long time (beyond 30 min) resulted in 5-HMF yield decrease up to 70 % (120 min), which is because of 5-HMF transformation to byproducts. Alam *et al.* also reported the same trend, describing 5-HMF yield reduction to 41% in 4 h and LA yield elevation up to 9% [40].

4.3 Variation of catalyst loading

233234

235

236

237

238

239

240

241

242

243

244

245

246

247

248249

250

251

252

253

254

255

256

257

258

259

260

261

262

263

264

265

266

267

268

The IL catalyst is tested in 30 min at 130 °C in various concentrations relative to a fixed amount of glucose. Experimental findings show that the IL catalyst is more efficient in the 40 mol% loading (Figure 5). An additional amount of the catalyst beyond the optimized 40 mol% causes a small

decrease in the 5-HMF yield. The optimization shows adding extra IL will not improve the catalytic

efficiency. The IL catalytic versus solvation behaviors were studied in our previous works [33, 34]. As previously explained, interintramolecular hydrogen bonds trap the catalytic spots (See Figure 1) in the presence of the bulk IL. Instead of the desired proton exchange with the molecules, interaction probability (hydrogen bonding) of the available oxygen and nitrogen atoms with protons increases considerably between the IL molecules. Declining the catalytic efficiencies beyond 40% of the IL loading can account for such intermolecular hydrogen bonding. Excess IL concentration may promote further dehydration of 5-HMF to byproducts. However, the formation of levulinic acid was not confirmed by UV-vis analysis. The glucose conversion to humin may be one of the possibilities in the presence of higher IL concentration. We carried out further

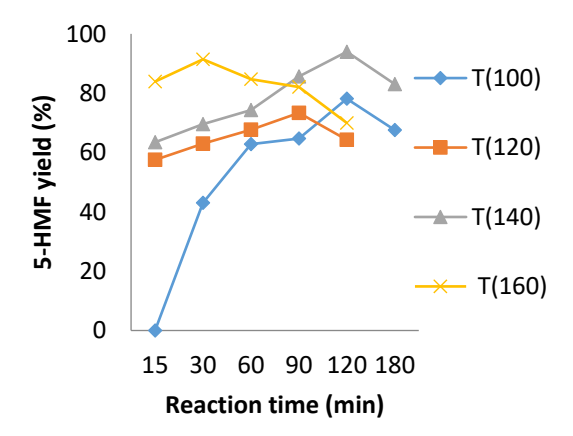


Figure 4. 5-HMF yields versus time at different temperatures (100-160 $^{\circ}$ C) in the presence of 30 mol% IL catalyst.

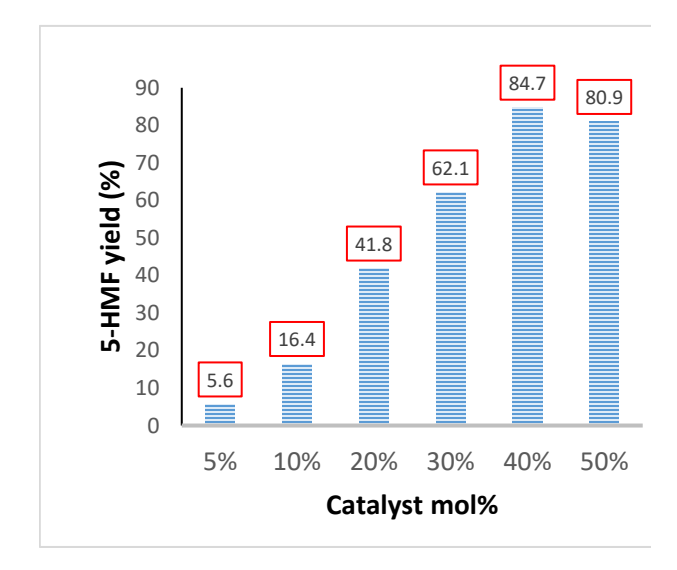


Figure 5. 5-HMF yield versus the IL catalyst loading at 130 °C after 30 min.

optimizations with 30 mol% catalyst (considering the economic concerns) to show that the catalyst can be utilized in lower quantities to reach a near quantitive 5-HMF yield.

4.4 Variation of solvents

We tested various solvents in the presence of 30 mol% [DPhDA]HSO₄ at 130 °C in 30 minutes (Figure 6). Reactions with dioxane and water were carried out at a reflux temperature. Nonpolar (dioxane (ϵ =2.2) and ethylbenzene (ϵ =2.4)) and polar (DMF (ϵ =37.2), DMA (ϵ =37.8), DMSO (ϵ =46.7), and water (ϵ =78.4)) solvents were chosen to investigate the 5-HMF yield versus solvent polarity. Studies show that the yield of 5-HMF increases with increasing static dielectric constant of solvents up to 46.7. Approximately

doubled the DMSO ε value resulted in the six-fold decrease of the 5-HMF yield. Therefore, DMSO was chosen as an ideal solvent for the α -glucose dehydration. The 5-HMF very low yields in the nonpolar solvent medium can be scrutinized with the solvation of substrate and the IL catalyst. Glucose and the IL are not soluble in dioxane and ethylbenzene, which resulted in poor interaction between the substances. DMF and DMA can dissolve the starting components upon heating, causing a considerable increase in the 5-HMF yield. Shifting to the DMSO and water, both capable of solvating the components properly at room temperature show dissimilar 5-HMF yield results. It can be rationalized with the formed 5-HMF stability in DMSO, whereas water promotes further rehydration of 5-HMF to the side products (e.g., levulinic acid, formic acid), consequently lower 5-HMF yield [35].

4.5 Recycle test

269

270

271

272

273

274

275

276

277

278

279

280

281

282

283

284

285

286

287

288

289

290

291

292

293

294

295

296

297

298

299

300

301

302

303

304

305

306

307

308

309

To display the effectiveness of IL [DPhDA]HSO₄ catalyst, we conducted a recycle test via carrying out five runs of the experiment, each with a 30 min reaction time at 160 °C. After each run, 5-HMF was extracted with diethyl ether carefully, and then the remaining residue was controlled with UV-vis analysis to ensure the vanishing 5-HMF and glucose signals. Fresh glucose was added to the catalyst/DMSO mixture for the next run. As seen from Figure 7, the IL catalyst can be utilized for the three consecutive runs without a decrease 5-HMF significant in vield. Accumulation of humin (it was not quantified, the elevation of viscosity, and darkness of the

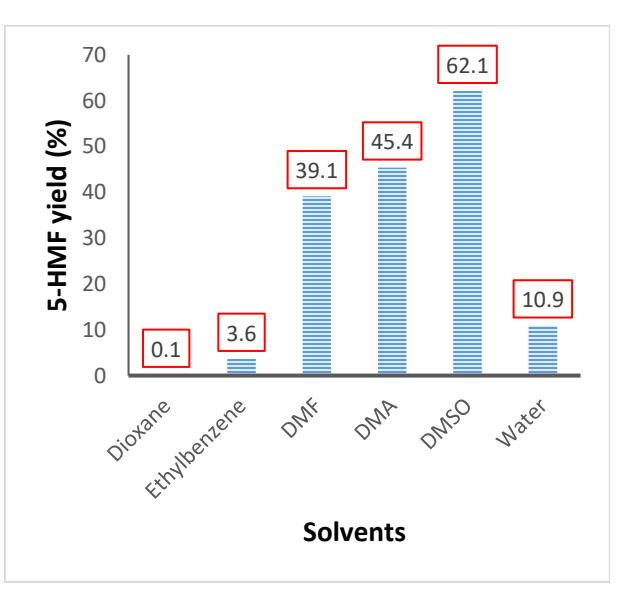


Figure 6. 5-HMF yield versus applied solvents at 130 °C after 30 min. Reflux condition was applied for dioxine and water media.

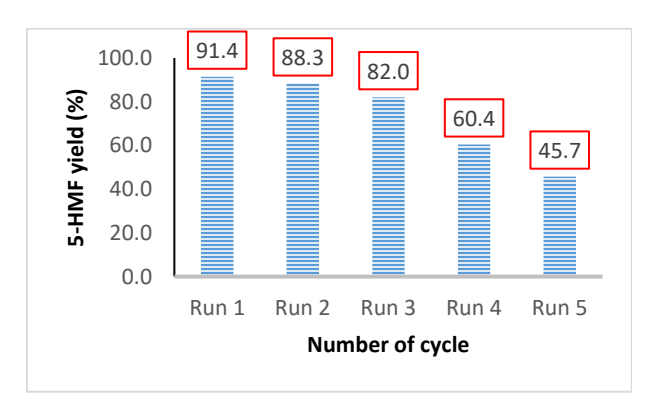


Figure 7. Reaction conditions: T =160 $^{\circ}$ C, time=30 min, solvent=DMSO, and catalyst=30 mol% [DPhDA]HSO₄. After extraction, the reaction mixture was heated to 70 $^{\circ}$ C under vacuum to remove residual diethyl ether and water.

reaction mixture indicates accumulated humin) from each experiment does not influence glucose conversion to 5-HMF but causes some difficulties in 5-HMF separation. The recycle test becomes

problematic, particularly in the last runs, and causes a large amount of extractive solvent consumption that needs to be addressed. The test verified that the utilized catalyst is comparable to the previously employed IL based homogeneous catalysts [26, 35], but we still have some drawbacks to achieve the heterogeneous catalyst performance in term of the catalyst reuse [41].

4.6 Mechanistic studies

310 311

312

313

314

315

316

317

318

319

320

321

322

323

324

325

326

327

328

329

330

331

332

333

334

335

336

337

338

339

340

We chose α -glucose as the starting compound for the mechanistic studies since its formation Gibbs energy is 4 kcal lower than for β -glucose and 14.6 kcal lower than for the open-chain glucose (I1) conformers. As seen from the energy profile (Figure 8), α -glucose ring-opening (TS1) occurs via a 20.4 kcal/mol barrier. In

most previous mechanistic studies [37, 42], it was suggested that α glucose is isomerized to the openchain conformer and then reisomerized to fructose, which dehydrated to 2,5-anhydromannose (I2A or I2C) as a three-step process. Marullo et al. transformed glucose to fructose (ca. 50% yield) and then performed the second experiment for the fructose dehydration to 5-HMF [43]. This study did not consider the possibility of the direct conversion of glucose to dehydrated fructose (I2A). Lower fructose yield may be an indication of the formation of the derivatives. Our fructose computations show that open-chain glucose can convert directly to 2,5anhydromannose via water extrusion: a five-membered ring formation and

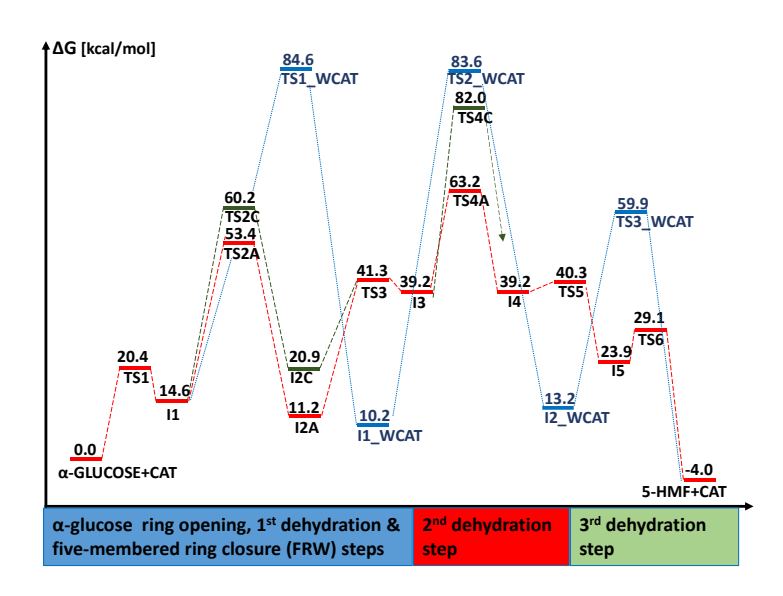


Figure 8. Gibbs energy profile of the IL (DPhDA]HSO₄, **CAT**) catalyzed α -glucose conversion to 5-HMF. TSs and intermediate names contain **WCAT** (without catalyst), which shows passive incorporation of the catalyst to the species in blue route.

water extrusion (FRW) take place simultaneously in a one concerted TS (**TS1_WCAT, TS2A**, and **TS2C**). The isomerization step to fructose is skipped since it is not efficient according to the experimental studies [43,

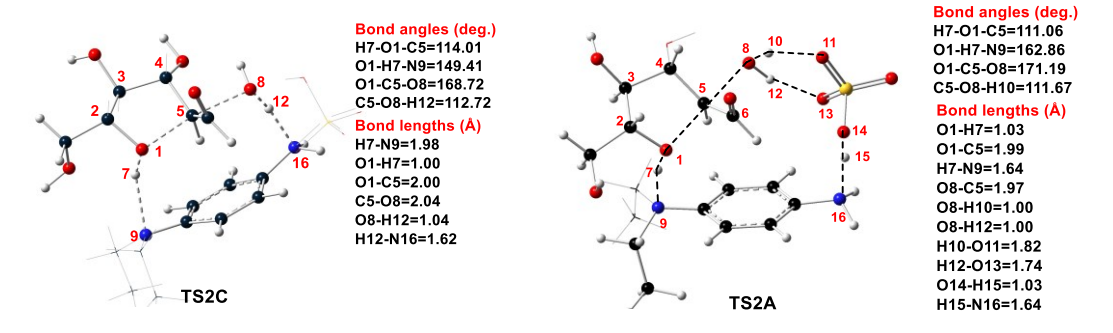


Figure 9. The five-membered ring closure and water extrusion (FRW) step TSs with important bond lengths (Å) and angles (deg.). **TS2C**: The IL cation part promoted TS. **TS2A**: The IL anion and cation parts promoted TS. Ethyl groups, some hydrogen atoms, and HSO_4^- are omitted to avoid clutter.

44]. The FRW step is possible without active incorporation of the catalyst via a high energy barrier (TS1_WCAT, 70 kcal/mol, See SI for the optimized structure). The catalytic IL interaction decreases the energy barrier of the crucial FRW step (Figure 9): The IL cation component can take part in proton exchange (TS2C). The basic spot of the cation (tertiary nitrogen atom: N9) abstracts proton (H7) over 1.98 Å bond length. At the same time, the acidic end (N16) donates a proton (H12) to hydroxyl via 1.62 Å elongation that results in water removal. The cation amphiprotic nature plays an essential role in TS2C via 45.6 kcal/mol energy barrier. The concerted FRW energy barrier is about 6 kcal less than the reported (calculated by B3PW91 functional) fructose first dehydration barrier catalyzed by imidazolium-based IL[28]. The basic part of the IL plays the same role as a proton abstractor, but the acidic end is replaced with HSO₄ in TS2A. The IL cation and anion components synchronized effects resulted in an even smaller barrier (38,8 kcal/mol, red route in Figure 8) relative to the TS2C and TS1 WCAT for the FRW step. Based on the investigations mentioned above, we propose the red route as the best catalytic option for the ratecontrolling FRW. The next step is the sp³-s C-H bond cleavage of C5 (See SI, Figure S1 for the TS3 structure). The energy barrier for this step is calculated to be 30.1 kcal/mol. The second dehydration step is observed to be 24 kcal/mol with the IL anion component proton donation (TS4A). The same step is possible with the IL cation component support via relatively high energy (TS4C, 42.8 kcal/mol). TS2_WCAT is also responsible for the catalyst-free concerted second dehydration and deprotonation step through a very high barrier (73.4 kcal/mol) relative to I1_WCAT. The remaining two catalytic steps (red route) are quite straightforward over shallow barriers to reach the fully annulated 5-HMF: the third dehydration step is calculated to be almost barrierless (TS5, 1.1 kcal/mol, See SI Figure S1) to reach I5, which yields 5-HMF through sp³-s C-H bond cleavage on C2 (TS6, 5.2 kcal/mol). The third catalyst-free concerted dehydration

341342

343

344

345346

347

348

349

350

351

352

353

354 355

356

357

358 359

360

361

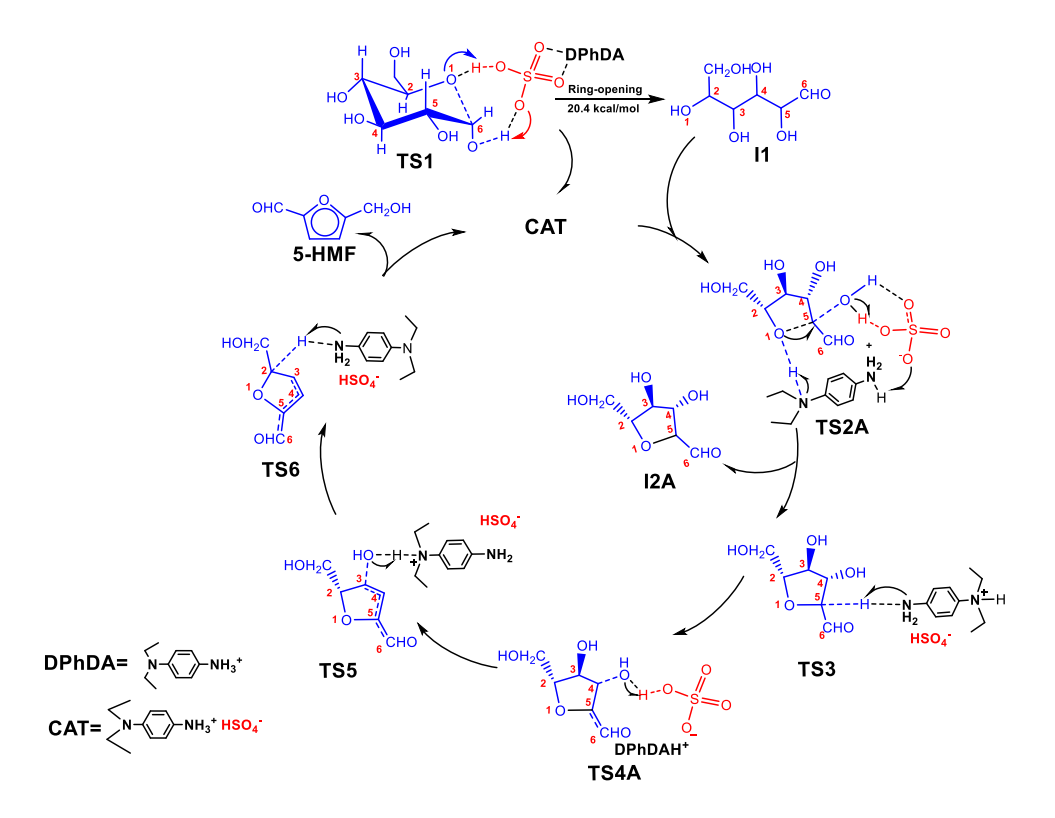


Figure 10. Calculated mechanism of the α -glucose dehydration to 5-HMF. Some intermediate structures are not shown for the sake of clarity.

and deprotonation step (**TS3_WCAT**) is also conceivable via the 46.7 kcal/mol barrier to release water and **5-HMF**. Our computation suggests the following mechanism (Figure 10) based on the shallow energy barriers (red route) of Figure 8.

5. Conclusions

362

363

364

365

366

367368

369

370

371

372

373

374

375

376

377

378

379

380

381

382

383

384

386

391

392

"Greener" and quantitative α -glucose conversion to 5-HMF (91.4% yield at 160 $^{\circ}$ C in 30 minutes) was carried out in the presence of the low-cost [DPhDA]HSO4 IL. Optimized reaction conditions show that increasing catalyst loading up to 40 mol% was beneficial for the 5-HMF yield elevation at 130 °C in 30 min. Polar aprotic solvents (DMF, DMA, and DMSO) were observed to be better for the α -glucose dehydration reaction compared to nonpolar solvents (dioxane, ethylbenzene). Inspired by the high 5-HMF yield, the IL catalyst structure was studied computationally with the NBO method (Figure 1). The identified catalytic spots were employed in the α -glucose dehydration mechanism (Figure 8 and Figure 10). Compared to the catalyst-free route (blue) energy barriers (three consecutive dehydration steps: TS1 WCAT, 70.0 kcal/mol; TS2_WCAT, 73.4 kcal/mol; TS3_WCAT, 46.7 kcal/mol), the IL catalyst proton exchanges with the substate molecule resulted in the considerable decline (almost double) in the concerted five-membered ring formation and water extrusion (FRW) TS energy barrier (TS2A, 38.8 kcal/mol). In return to the higher energy remaining two catalyst-free steps (TS2_WCAT, TS3_WCAT), we calculated four catalytic steps with not too high energy barriers (TS3, 30.1 kcal/mol; TS4A, 24 kcal/mol; TS5,1.1 kcal/mol; TS6, 5.2 kcal/mol) to achieve the 5-HMF formation. Other possible catalytic steps (TS2C, TS4C; green route, Figure 8) were also calculated for the dehydration mechanism. The huge gap between the energies of the catalyst-free and catalytic routes showed the IL catalytic influences on the studied reaction. We believe this study will draw attention to exploring new environmentally benign IL catalysts for the biomass valorization processes.

Conflicts of interest

385 The authors declare no conflicts of interest.

Acknowledgments

Y.A. acknowledges the financial support from the BP Azerbaijan (grant-CW2192142) and the SOCAR Science Foundation, S/N 17LR-AMEA. The authors thank the Center for Computational Research (CCR) at the University at Buffalo for providing computational resources. JA acknowledges support from grant CHE-1855740 from the National Science Foundation.

References

- Mittal A, Pilath HM, Johnson DK. Direct Conversion of Biomass Carbohydrates to Platform Chemicals: 5-Hydroxymethylfurfural (HMF) and Furfural. Energy & Fuels 2020;34(3):3284-93.
- Alam MI, De S, Khan TS, Haider MA, Saha B. Acid functionalized ionic liquid catalyzed transformation of non-food biomass into platform chemical and fuel additive. Industrial Crops and Products 2018;123:629-37.
- 398 [3] Branco-Vieira M, Mata TM, Martins AA, Freitas MAV, Caetano NS. Economic analysis of microalgae biodiesel production in a small-scale facility. Energy Reports 2020;6:325-32.
- 400 [4] Qian Y, Zhu L, Wang Y, Lu X. Recent progress in the development of biofuel 2,5-dimethylfuran.
 401 Renewable and Sustainable Energy Reviews 2015;41:633-46.

- 402 [5] Yu X, Gao X, Peng L, He L, Zhang J. Intensified 5-Ethoxymethylfurfural Production from Biomass 403 Components over Aluminum-Based Mixed-Acid Catalyst in Co-Solvent Medium. ChemistrySelect 404 2018;3(47):13391-9.
- 405 [6] Xiao B, Zheng M, Li X, Pang J, Sun R, Wang H, et al. Synthesis of 1,6-hexanediol from HMF over double-layered catalysts of Pd/SiO2 + Ir–ReOx/SiO2 in a fixed-bed reactor. Green Chemistry 2016;18(7):2175-84.
- 408 [7] Brandolese A, Ragno D, Di Carmine G, Bernardi T, Bortolini O, Giovannini PP, et al. Aerobic 409 oxidation of 5-hydroxymethylfurfural to 5-hydroxymethyl-2-furancarboxylic acid and its 410 derivatives by heterogeneous NHC-catalysis. Organic & Biomolecular Chemistry 411 2018;16(46):8955-64.
- Koopman F, Wierckx N, de Winde JH, Ruijssenaars HJ. Efficient whole-cell biotransformation of 5-(hydroxymethyl)furfural into FDCA, 2,5-furandicarboxylic acid. Bioresource Technology 2010;101(16):6291-6.
- Rosenboom J-G, Hohl DK, Fleckenstein P, Storti G, Morbidelli M. Bottle-grade polyethylene furanoate from ring-opening polymerisation of cyclic oligomers. Nat Commun 2018;9(1):2701.
- 417 [10] Fachri BA, Abdilla RM, Rasrendra CB, Heeres HJ. Experimental and modelling studies on the 418 uncatalysed thermal conversion of inulin to 5-hydroxymethylfurfural and levulinic acid. 419 Sustainable Chemical Processes 2015;3(1):8.
- 420 [11] Ginés-Molina MJ, Ahmad NH, Mérida-Morales S, García-Sancho C, Mintova S, Eng-Poh N, et al.
 421 Selective Conversion of Glucose to 5-Hydroxymethylfurfural by Using L-Type Zeolites with
 422 Different Morphologies. Catalysts 2019;9(12).
- 423 [12] Istasse T, Lemaur V, Debroux G, Bockstal L, Lazzaroni R, Richel A. Monosaccharides Dehydration
 424 Assisted by Formation of Borate Esters of α-Hydroxyacids in Choline Chloride-Based Low Melting
 425 Mixtures. Frontiers in Chemistry 2020;8(569).
- 426 [13] de Melo FC, Bariviera W, Zanchet L, de Souza RF, de Souza MO. C10MI·CF3SO3: a hydrophobic
 427 ionic liquid medium for the production of HMF from sugars avoiding the use of organic solvent.
 428 Biomass Conversion and Biorefinery 2020;10(2):611-8.
- Tosi I, Elliot SG, Jessen BM, Riisager A, Taarning E, Meier S. Uncharted Pathways for CrCl3 Catalyzed Glucose Conversion in Aqueous Solution. Topics in Catalysis 2019;62(7):669-77.
- 431 [15] Elsayed I, Mashaly M, Eltaweel F, Jackson MA, Hassan EB. Dehydration of glucose to 5-432 hydroxymethylfurfural by a core-shell Fe3O4@SiO2-SO3H magnetic nanoparticle catalyst. Fuel 433 2018;221:407-16.
- Hu L, Sun Y, Lin L. Efficient Conversion of Glucose into 5-Hydroxymethylfurfural by Chromium(III)
 Chloride in Inexpensive Ionic Liquid. Ind Eng Chem Res 2012;51(3):1099-104.
- 436 [17] Yang Y, Liu W, Wang N, Wang H, Song Z, Li W. Effect of organic solvent and Brønsted acid on 5-437 hydroxymethylfurfural preparation from glucose over CrCl3. RSC Advances 2015;5(35):27805-438 13.
- 439 [18] Yuan Z, Xu C, Cheng S, Leitch M. Catalytic conversion of glucose to 5-hydroxymethyl furfural using inexpensive co-catalysts and solvents. Carbohydrate Research 2011;346(13):2019-23.
- 441 [19] Qi X, Watanabe M, Aida TM, Smith Jr RL. Fast Transformation of Glucose and Di-442 /Polysaccharides into 5-Hydroxymethylfurfural by Microwave Heating in an Ionic Liquid/Catalyst 443 System. ChemSusChem 2010;3(9):1071-7.
- Eminov S, Brandt A, Wilton-Ely JDET, Hallett JP. The Highly Selective and Near-Quantitative Conversion of Glucose to 5-Hydroxymethylfurfural Using Ionic Liquids. PLOS ONE 2016;11(10):e0163835.
- Guo H, Duereh A, Hiraga Y, Qi X, Smith RL. Mechanism of Glucose Conversion into 5-Ethoxymethylfurfural in Ethanol with Hydrogen Sulfate Ionic Liquid Additives and a Lewis Acid Catalyst. Energy & Fuels 2018;32(8):8411-9.

- 450 [22] Yang Y, Hu C, Abu-Omar MM. The effect of hydrochloric acid on the conversion of glucose to 5-451 hydroxymethylfurfural in AlCl3–H2O/THF biphasic medium. Journal of Molecular Catalysis A: 452 Chemical 2013;376:98-102.
- Yang Y, Hu C, Abu-Omar MM. Conversion of glucose into furans in the presence of AlCl3 in an ethanol—water solvent system. Bioresource Technology 2012;116:190-4.
- Liu X, Afzal W, He M, Prausnitz JM. Solubilities of small hydrocarbons, viscosities of diluted tetraalkylphosphonium bis(2,4,4-trimethylpentyl) phosphinates. AIChE Journal 2014;60(7):2607-12.
- 458 [25] Qu Y, Huang C, Song Y, Zhang J, Chen B. Efficient dehydration of glucose to 5-459 hydroxymethylfurfural catalyzed by the ionic liquid,1-hydroxyethyl-3-methylimidazolium 460 tetrafluoroborate. Bioresource Technology 2012;121:462-6.
- 461 [26] Ramli NAS, Amin NAS. A new functionalized ionic liquid for efficient glucose conversion to 5-462 hydroxymethyl furfural and levulinic acid. Journal of Molecular Catalysis A: Chemical 463 2015;407:113-21.
- Shi X-L, Zhang M, Li Y, Zhang W. Polypropylene fiber supported ionic liquids for the conversion of fructose to 5-hydroxymethylfurfural under mild conditions. Green Chemistry 2013;15(12):3438-45.
- Li J, Yang Y, Zhang D. DFT study of fructose dehydration to 5-hydroxymethylfurfural catalyzed by imidazolium-based ionic liquid. Chemical Physics Letters 2019;723:175-81.
- Li Y-N, Wang J-Q, He L-N, Yang Z-Z, Liu A-H, Yu B, et al. Experimental and theoretical studies on imidazolium ionic liquid-promoted conversion of fructose to 5-hydroxymethylfurfural. Green Chemistry 2012;14(10):2752-8.
- 472 [30] Arora JS, Chew JW, Mushrif SH. Influence of Alkali and Alkaline-Earth Metals on the Cleavage of 473 Glycosidic Bond in Biomass Pyrolysis: A DFT Study Using Cellobiose as a Model Compound. The 474 Journal of Physical Chemistry A 2018;122(38):7646-58.
- 475 [31] Mayes HB, Broadbelt LJ. Unraveling the Reactions that Unravel Cellulose. The Journal of Physical Chemistry A 2012;116(26):7098-106.
- Wang Q, Fu M, Li X, Huang R, Glaser RE, Zhao L. Aluminum alkoxy-catalyzed biomass conversion of glucose to 5-hydroxymethylfurfural: Mechanistic study of the cooperative bifunctional catalysis. J Comput Chem 2019;40(16):1599-608.
- 480 [33] Abdullayev Y, Abbasov V, Ducati LC, Talybov A, Autschbach J. Ionic Liquid Solvation versus
 481 Catalysis: Computational Insight from a Multisubstituted Imidazole Synthesis in [Et2NH2][HSO4].
 482 ChemistryOpen 2016;5(5):460-9.
- Valiyev I, Abdullayev Y, Yagubova S, Baybekov S, Salmanov C, Autschbach J. Experimental and computational study of metal-free Brønsted acidic ionic liquid catalyzed benzylic C(sp3)H bond activation and CN, CC cross couplings. Journal of Molecular Liquids 2019;280:410-9.
- 486 [35] De S, Dutta S, Saha B. Microwave assisted conversion of carbohydrates and biopolymers to 5-487 hydroxymethylfurfural with aluminium chloride catalyst in water. Green Chemistry 488 2011;13(10):2859-68.
- Frisch MJ, Trucks GW, Schlegel HB, Scuseria GE, Robb MA, Cheeseman JR, et al. Gaussian 16, Revision C.01. Gaussian Inc. Wallingford CT; 2016.
- 491 [37] Arora JS, Ansari KB, Chew JW, Dauenhauer PJ, Mushrif SH. Unravelling the catalytic influence of 492 naturally occurring salts on biomass pyrolysis chemistry using glucose as a model compound: a 493 combined experimental and DFT study. Catalysis Science & Technology 2019;9(13):3504-24.
- Chiappe C, Rajamani S, D'Andrea F. A dramatic effect of the ionic liquid structure in esterification reactions in protic ionic media. Green Chemistry 2013;15(1):137-43.
- 496 [39] Xiao L, Su D, Yue C, Wu W. Protic ionic liquids: A highly efficient catalyst for synthesis of cyclic carbonate from carbon dioxide and epoxides. Journal of CO2 Utilization 2014;6:1-6.

- 498 [40] Alam MI, De S, Singh B, Saha B, Abu-Omar MM. Titanium hydrogenphosphate: An efficient dual 499 acidic catalyst for 5-hydroxymethylfurfural (HMF) production. Applied Catalysis A: General 500 2014;486:42-8. 501 [41] Zhao P, Zhang Y, Wang Y, Cui H, Song F, Sun X, et al. Conversion of glucose into 5-502 hydroxymethylfurfural catalyzed by acid-base bifunctional heteropolyacid-based ionic hybrids. 503 Green Chemistry 2018;20(7):1551-9. 504 [42] Qiu G, Huang C, Sun X, Chen B. Highly active niobium-loaded montmorillonite catalysts for the 505 production of 5-hydroxymethylfurfural from glucose. Green Chemistry 2019;21(14):3930-9. 506 [43] Marullo S, Sutera A, Gallo G, Billeci F, Rizzo C, D'Anna F. Chemo-enzymatic Conversion of
 - [43] Marullo S, Sutera A, Gallo G, Billeci F, Rizzo C, D'Anna F. Chemo-enzymatic Conversion of Glucose in 5-Hydroxymethylfurfural: The Joint Effect of Ionic Liquids and Ultrasound. ACS Sustainable Chemistry & Engineering 2020;8(30):11204-14.

507

508

512

509 [44] Marianou AA, Michailof CM, Pineda A, Iliopoulou EF, Triantafyllidis KS, Lappas AA. Glucose to 510 Fructose Isomerization in Aqueous Media over Homogeneous and Heterogeneous Catalysts. 511 ChemCatChem 2016;8(6):1100-10.